N84-32435

NASA Technical Memorandum 86287

HOLE INTERACTION AND LOAD INTRODUCTION EFFECTS FOR COMPRESSION-LOADED LAMINATES WITH HOLES

MARK J. SHUART

AUGUST 1984

National Aeronautics and Space Administration

Langley Research Center
Hampton, Virginia 23665

HOLE INTERACTION AND LOAD INTRODUCTION EFFECTS FOR COMPRESSION-LOADED LAMINATES WITH HOLES

By

Mark J. Shuart*
Structures and Dynamics Division
NASA Langley Research Center
Hampton, VA 23665

ABSTRACT

An experimental investigation of a hole interaction effect and a load introduction effect for $[(\pm30/90)_8]_s$ and $[(\pm45)_{12}]_s$ laminates with holes was conducted. A hole interaction region was identified in some specimens, and this region was ineffective for carrying load. The membrane stiffness of a specimen with a hole interaction region is less than the membrane stiffness of a similar specimen without a hole interaction region. A load introduction effect that occurs on the sublaminate level was also observed. This effect can cause a non-uniform load diffusion into the interior of the specimen.

INTRODUCTION

The response and failure characteristics of composite laminates must be understood to design reliable, efficient composite structures. For example, the behavior of laminates with discontinuities is being widely studied. Experimental results of compression-loaded composite laminates have shown that severe reductions in failure strain can occur due to local discontinuities such as holes (ref. 1). The data in reference 1 are for orthotropic and quasi-isotropic specimens that can be described as fiber-dominated, i.e., the specimens had 0^{o} fibers parallel to the loading direction, and the plies containing these fibers

---

* Aerospace Engineer, Structural Mechanics Branch.

governed the specimen response. The effect of a hole on the compression failure strain of $[(45)_{12}]_s$ laminates has also been studied (ref. 2). The failure strain for a $[(\pm45)_{12}]_s$ laminate with a hole was found to be higher than the failure strain for a fiber-dominated, quasi-isotropic laminate with a similar hole. The failure mode for these $[(\pm45)_{12}]_s$ specimens was not the same as the failure mode for the quasi-isotropic specimens. A failure prediction technique (ref. 3) has been applied to compression-loaded laminates with a hole for a variety of laminate orientations and specimen geometries (ref. 4). The results from reference 4 showed excellent correlation between predicted and experimental compression failure strains for fiber-dominated laminates. However, the experimental failure strain for some $[(\pm30/90)_8]_s$ laminates did not agree with the prediction. The compression strength for this laminate was described as being controlled by mechanisms other than filament strength.

The $[(\pm45)_{12}]_s$ and $[(\pm30/90)_8]_s$ laminates have angle plies as the principal load-carrying layers. Because of these plies, load diffusion in the laminates is governed by inplane shearing mechanisms that occur on a sublaminate level. For this report, laminates that have such mechanisms are described as shear-dominated. Load diffusion in fiber-dominated laminates is governed by the behavior of the 0^o plies. The failure strain for a shear-dominated laminate with a hole may be different from the failure strain for a fiber-dominated laminate with a similar hole because of the different sublaminate load diffusion mechanisms.

The current investigation was conducted to study the strain distribution in the center of shear-dominated laminates with holes and to determine the cause of differences between experimental and predicted failure strains for $[(\pm30/90)_8]_s$ laminates with a hole; results of this investigation are reported herein. Data are presented for $[(\pm30/90)_8]_s$ graphite-epoxy laminates with one or two holes and for $[(\pm45)_{12}]_s$ graphite-epoxy laminates with two holes. The effect of hole interaction on laminate response for $[(\pm30/90)_8]_s$ and $[(\pm45)_{12}]_s$ laminates with two holes is discussed. The interaction between the load diffusion into the laminate and the load distribution around the hole is described for these laminates. The compression failure strains for a quasi-isotropic $[(\pm30/90)_8]_s$ laminate with a single hole are compared to the compression failure strains for a fiber-dominated, quasi-isotropic $[0/\pm45/90]_s$-class laminate with a similar hole.

TEST SPECIMENS

The graphite-epoxy composite specimens tested in this investigation were fabricated from commercially available unidirectional Hercules AS4 graphite fiber layers preimpregnated with 450K cure Hercules 3502 thermosetting epoxy resin. Each laminate contained 48 layers and was approximately 0.64 cm thick. The laminates were cured in an autoclave using the manufacturer's recommended procedure. Following cure, the laminates were ultrasonically C-scanned to establish specimen quality and then cut into test specimens. All specimens were 12.7 cm wide by either 25.4 cm or 38.1 cm long. The loaded ends of each specimen were machined flat and parallel to permit uniform compression loading. Circular holes were machined into the specimens with diamond impregnated core drills. The stacking sequence and geometry for each specimen are given in Table 1.

The specimen geometry is symmetric with respect to the horizontal centerline and the vertical centerline. Hole centers are located using the distance from the specimen edge e (edge distance) and the distance between centers a as shown in Table 1. Only e is needed to describe the hole location for specimens with one hole. Results for specimens with one hole are presented using e. Either e or a can be used to describe the specimen geometry for specimens of the same length with two holes. For consistency, results for specimens with two holes are also presented using e.

Identification of commercial products and companies in this report is used to describe adequately the test materials. The identification of these commercial products does not constitute endorsement, expressed or implied, of such products by the National Aeronautics and Space Administration.

APPARATUS AND TESTS

Test specimens were loaded in axial compression using a 1.33-MN capacity hydraulic testing machine. The loaded ends of the specimen were clamped by fixtures during testing, and the sides were simply supported by restraints to prevent the specimen from buckling as a wide column. A typical specimen with two holes is shown mounted in the support fixture in figure 1.

Electrical resistance strain gages were used to monitor strains, and direct-current differential transformers were used to monitor longitudinal displacements of the ends. Electrical signals from the instrumentation and the corresponding applied loads were recorded on magnetic tape at regular time intervals during the test.

All specimens were tested to failure by quasi-statically applying a compressive load. The $[(\pm 30/90)_8]_s$ specimens had either one or two holes (see Table 1). The holes had diameters ranging from 1.27 cm to 5.08 cm and were located on the centerline parallel to the specimen side at distances ranging from 5.08 cm to 19.05 cm from the specimen end. All $[(\pm 45)_{12}]_s$ specimens had two holes. The holes had either 1.27 cm or 2.54 cm diameters and were located on the centerline parallel to the specimen side at either 6.35 cm or 7.62 cm from the specimen end. All 25.4-cm-long specimens had holes that were located to intersect fibers beginning at the specimen end. Fibers beginning at the specimen end did not intersect the holes in the 38.1-cm-long specimens. One specimen was tested for each configuration. A total of fifteen specimens were tested.

RESULTS AND DISCUSSION

This section presents experimental results for $[(\pm30/90)_8]_s$ laminates and for $[(\pm45)_{12}]_s$ laminates. Failure is discussed for each laminate stacking sequence. A hole interaction effect is discussed using the strain distribution in the center of the laminate at failure. The membrane stiffness EA as a function of specimen geometry is described for the $[(\pm30/90)_8]_s$ specimens. Membrane stiffness data for the $[(\pm45)_{12}]_s$ specimens were not obtained due to the nonlinear behavior of this laminate. A load introduction effect is described. Far-field laminate stress and strain data at failure as a function of specimen geometry are presented.

$[(\pm30/90)_8]_s$ Laminates

Typical stress-strain behavior for a region near the edge of a hole in a $[(\pm30/90)_8]_s$ laminate is shown in figure 2a. Failure of these laminates with holes is defined in this investigation as the first local failure event that occurs at the edge of the hole as indicated by a sharp discontinuity in this stress-strain curve (figure 2a). In this report, the failure stress is the far-field laminate stress when the first local failure event occurs. The failure strain is calculated using the specimen end-shortening at the failure stress and the initial specimen length. Failure stress and strain data are reported in Table 2. The specimen continues to carry load after the first local failure event while additional local failure events occur. A typical region of local failure close to the hole is shown by the radiograph in figure 2b. An X-ray opaque dye was applied at the edge of the hole. The dye penetrated into any crack or delamination and enhanced the image of the local failure region. The maximum load-carrying capability of a specimen occurs when the region of local failure propagates across the specimen width.

Hole Interaction Effect

The axial strain at failure along the y-axis (x = 0) in figure 3 is shown for specimens with two 1.27-cm-diameter holes. The strain data are normalized by the far-field axial strain at failure. The axial strain along x = 0 is a measure of load diffusion into the region between the holes. For example, for e/d = 4.0 (specimen A6, triangular symbols), the strain at the center of the specimen is the same as the far-field strain. The load is diffused around the hole and is uniformly distributed in the center of the laminate. For this specimen the holes are independent of each other. However, for e/d = 7.5 and e/d = 8.5 (specimen A7, square symbols and specimen A9, circular symbols, respectively), the strain at the center of the specimen is less than the far-field strain, and the load is diffused away from the center of the laminate. For these specimens, the holes appear to interact.

The axial strain along the y-axis (x = 0) at failure normalized by the far-field axial strain at failure is shown in figure 4 for specimens with two 2.54-cm-diameter holes. Data for e/d = 2.0 (specimen A10) and for e/d = 3.5 (specimen A11) are plotted using square and circular symbols, respectively. In both cases the strain in the center of the specimen is less than the far-field strain indicating that the load is diffused away from the center of the laminate. For these specimens also, the holes appear to interact.

These strain data for specimens with two holes show that the stress field around one hole may interact with the stress field around the other hole to diffuse load away from the region between the holes. In this report, this effect on the load diffusion is referred to as a hole interaction effect. The hole interaction effect is a function of hole diameter and hole location. When this effect occurs, the inplane area between the holes can be described as the hole interaction region. The distance between the hole centers (a in Table 1) is a measure of the size of the hole interaction region. Hole interaction has been observed for isotropic plates with two holes and has been shown to affect the stress trajectories in such plates (ref. 5). Load is diffused away from the centers of specimens A7, A9, A10, and A11 due to hole interaction, and this behavior suggests that the hole interaction region is ineffective for carrying load.

Laminate membrane stiffness EA was measured for each $[(\pm 30/90)_8]_s$ specimen with holes and is reported in Table 2. The membrane stiffness was obtained using the slope of the load-shortening curve for each specimen. The load-shortening response for this laminate was linear to failure. The membrane stiffness of specimens with holes is shown as a function of the edge-distance-to-hole-diameter ratio e/d in figure 5. Data are plotted for specimens having 1.27-cm- and 2.54-cm-diameter holes. The open and closed symbols are data for specimens with a single hole and with two holes, respectively. For the specimens with 1.27-cm-diameter holes, EA decreases to a minimum at e/d = 8.5 and then increases as e/d increases (i.e., as the holes get closer together). However, for the specimens with 2.54-cm-diameter holes EA only increases as e/d increases. The strain data for specimens with 1.27-cm-diameter holes show that a specimen with small e/d (e.g., specimen A6, e/d = 4.0) does not have a hole interaction effect because the holes are far apart. Increasing e/d (i.e., moving the holes closer together) results in a hole interaction effect which decreases the membrane stiffness to a minimum at approximately e/d = 8.5. The membrane stiffness decreases since the hole interaction region is ineffective for carrying load. Further increasing e/d (i.e., moving the holes still closer together until they merge into one hole) reduces and finally eliminates the hole interaction effect. The membrane stiffness increases to the value obtained for small e/d as the hole interaction effect is reduced. The data in figure 5 for specimens with 2.54-cm-diameter holes show only the EA response where increasing e/d reduces the hole interaction effect and, thus, increases the membrane stiffness. Hence, the membrane stiffness of a plate affected by hole interaction is less than the membrane stiffness of a plate that is not affected by hole interaction. The data in figure 5 illustrates the membrane stiffness is a useful property for studying the influence of hole interaction on laminate response.

Load Introduction Effect

Far-field strain at the maximum load as a function of the hole-diameter-to-plate-width ratio is presented in figure 6. All data in this figure were obtained from specimens with a single circular hole. Upper and lower bound on the failure strain based on notch insensitive and notch sensitive laminate behavior, respectively (ref. 6), are also shown in this figure. For comparison with a fiber-dominated laminate, the predicted failure strain based on analysis (line) and the data (circular symbols) are shown on the figure for a quasi-isotropic laminate taken from reference 4. The open and half-filled squares in figure 6 represent test results for 25.4-cm-long $[(\pm 30/90)_8]_s$ specimens, and some of these data are less than the established lower bound. This behavior may be due to a load introduction effect. The filled squares in figure 6 represent test results for 38.1-cm-long specimens, and these data agree with the failure prediction. These data indicate that the load introduction effect is eliminated by lengthening the specimen.

The load introduction effect is a function of specimen length, hole diameter, and ply orientation and can occur in shear-dominated laminates. This effect occurs on a sublaminate level and is illustrated in figure 7 for a $[\pm 30/90]_s$-class laminate with a single hole. For a 25.4-cm-long specimen with a 5.08-cm-diameter hole (figure 7a), a 30^o fiber beginning at the specimen corner intersects the hole before intersecting the specimen side causing a nonuniform load diffusion into the interior of the laminate. This effect is eliminated by lengthening the specimen as shown in figure 7b.

Far-Field Failure Strain

In addition to hole diameter, failure strain is also a function of the hole location. Far-field strain at failure is shown in figure 8 as a function of e/d. Data are plotted for specimens having 1.27-cm-diameter holes and for specimens having 2.54-cm-diameter holes. The open symbols are data for specimens with a single hole; the closed symbols are data for specimens with two holes. For the specimens with 1.27-cm-diameter holes (square symbols), the failure strain for e/d = 4.0 is the same as the failure strain for e/d = 10.0. These data suggest that the load introduction effect may have a negligible influence on the failure strain for specimens with 1.27-cm-diameter holes. However, the failure strain varies for e/d = 7.5, 8.0, and 8.5. This variation may be due to the hole interaction effect that was observed for these values of e/d. The failure strain for the specimens with 2.54-cm-diameter holes (circular symbols) increases as e/d increases. For example, the failure strain of these specimens is a minimum for e/d = 2.0 (specimen A10) and is a maximum for e/d = 7.5 (specimen A3). In addition to the hole interaction effect described above, specimen A10 may also be influenced by the load introduction effect. Specimen A3 has a single hole and is not influenced by the load introduction effect because a 30° fiber in this specimen intersects the specimen side before intersecting the hole.

$[(\pm45)_{12}]_s$ Laminates

A typical far-field stress-strain curve is shown in figure 9a for a specimen with two 1.27-cm-diameter holes. The behavior is nonlinear, and failure is labeled on the curve. Failure of $[(\pm45)_{12}]_s$ laminates with holes corresponds to near-zero slope of the far-field stress-strain curve. A typical failed specimen was C-scanned, and a photograph of the results is shown in figure 9b. Local failure is indicated by the white regions on the photograph. The C-scan results show $\pm 45^{\circ}$ bands of failure that extend from the hole boundary to the simply-supported edges. The primary compressive failure mechanism for this specimen appears to be the same matrix-shearing mechanism that was identified for $[(\pm 45)_{12}]_s$ laminates with a single circular hole in reference 2. The bands in figure 9b are described as matrix-shearing bands. Failure stress and strain data for the $[(\pm 45)_{12}]_s$ specimens are presented in Table 3. Membrane stiffness data were not obtained due to the nonlinear load-end shortening behavior for this laminate orientation.

The axial strain at failure along the y-axis (x = 0) in figure 10 is shown for a specimen with two 1.27-cm-diameter holes (specimen B1, square symbols) and for a specimen with two 2.54-cm-diameter holes (specimen B2, circular symbols). The strain data are normalized by the far-field axial strain at failure. The strain for specimen B1 is approximately constant across the width of the specimen and is within ten percent of the far-field strain. For this specimen the holes are independent of each other. The strain in the center of specimen B2 is less than the far-field strain. This behavior is the result of hole interaction.

Failure stress as a function of the edge-distance-to-hole-diameter ratio e/d is shown in figure 11. Failure stress is plotted instead of failure strain (cf., figure 8) since the failure stress is a more accurately-defined maximum value than the failure strain for this laminate orientation. Data for specimens having 1.27-cm-diameter holes and for specimens having 2.54-cm-diameter holes are plotted in figure 11 using square and circular symbols, respectively. The open symbols are data for specimens with a single hole (ref. 2), and the closed symbols are data for specimens with two holes. These limited data suggest that the laminate strength does not appear to be influenced by a load introduction effect. The load introduction effect may be a function of the inplane shear modulus since load diffusion in these laminates is governed by inplane shearing mechanisms. The inplane shear modulus for a $[(\pm 45)_{12}]_s$ laminate is greater than the inplane shear modulus for a $[(\pm 30/90)_8]_s$ laminate.

CONCLUDING REMARKS

An investigation of a hole interaction effect and a load introduction effect for $[(\pm 30/90)_8]_s$ and $[(\pm 45)_{12}]_s$ laminates with holes was conducted. These laminates were described in this study as shear dominated since load diffusion in these laminates is governed by inplane shearing mechanisms that occur on the sublaminate level. The $[(\pm 30/90)_8]_s$ specimens had one or two holes; all the $[(\pm 45)_{12}]_s$ specimens had two holes. The response of shear-dominated laminates with holes was sensitive to specimen geometry. The results of this investigation illustrate that effects on a sublaminate level influence the global laminate response.

A hole interaction effect that results from the stress field around one hole interacting with the stress field around another hole was identified for some specimens with two holes. The strain distribution in the center of these specimens showed that load was diffused away from the center of the laminate. This behavior was observed for both $[(\pm 30/90)_8]_s$ and $[(\pm 45)_{12}]_s$ specimens. The hole interaction region appeared to be ineffective for carrying load. The membrane stiffness of a specimen with a hole interaction region is less than the membrane stiffness of a similar specimen without a hole interaction region.

Differences between experimental and predicted failure strains for $[(\pm 30/90)_8]_s$ laminates with a hole were due to the load introduction effect. This effect occurred in some specimens of this laminate that were 25.4-cm-long causing a nonuniform load diffusion into the interior of the specimen. The effect was a function of specimen length, hole diameter, and ply orientation. Experimental results indicate that the effect was eliminated by lengthening the specimen. Limited experimental results suggest that the strength of $[(\pm 45)_{12}]_s$ laminates with holes was not affected by the load introduction effect.

REFERENCES

1. Starnes, J. H., Jr.; Rhodes, M. D.; and Williams, J. G.: Effect of Impact Damage and Holes on the Compressive Strength of a Graphite/Epoxy Laminate. Nondestructive Evaluation and Flaw Criticality for Composite Materials, ASTM STP 696, R. B. Pipes, ed., American Society for Testing and Materials, 1979, pp. 145-171.

2. Shuart, M. J.; and Williams, J. G.: Compression Failure Characteristics of $\pm 45^{\circ}$-Dominated Laminates with a Circular Hole or Impact Damage. AIAA Paper No. 84-0848, May 1984.

3. Whitney, J. M.; and Nuismer, R. J.: Stress Fracture Criteria for Laminated Composites Containing Stress Concentrations. Journal of Composite Materials, v. 8, July 1974, pp. 253-265.

4. Rhodes, M. D.; Mikulas, M. M., Jr.; and McGowan, P. E.: Effects of Orthotropy and Width on the Compression Strength of Graphite-Epoxy Panels with Holes. AIAA Journal, v. 22, no. 9, September 1984, pp. 1283-1292.

5. Savin, G. N. (Eugene Gros, transl.): Stress Concentration Around Holes. Pergamon Press, 1961.

6. Mikulas, M. M., Jr.: Failure Prediction Technique for Compressive Loaded Composite Laminates with Holes. Selected NASA Research in Composite Materials and Structures, NASA CP 2142, August 1980, pp. 1-33.

TABLE 1. SPECIMEN STACKING SEQUENCE AND GEOMETRY[1].

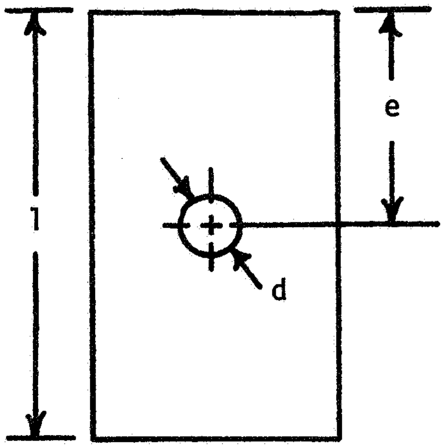

specimen with a single hole (a = 0)

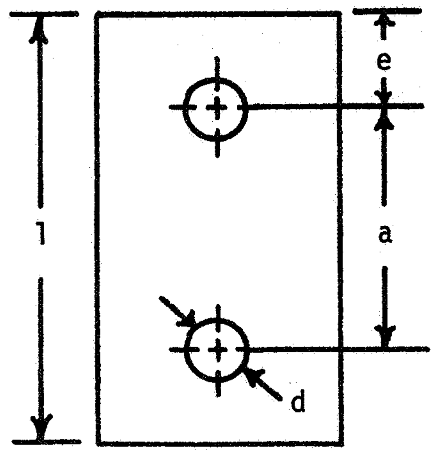

specimen with two holes

Specimen	Laminate Orientation	Laminate Thickness, cm	l, cm	d, cm	e, cm	a, cm
A1	$[(\pm30/90)_8]_s$	0.59	25.4	1.27	12.70	0.
A2	↓	.59	25.4	2.54	12.70	0.
A3		.67	38.1	2.54	19.05	0.
A4		.68	38.1	3.81	19.05	0.
A5		.68	38.1	5.08	19.05	0.
A6		.59	25.4	1.27	5.05	15.24
A7		.58	25.4	1.27	9.53	6.35
A8		.65	25.4	1.27	10.16	5.08
A9		.65	25.4	1.27	10.80	3.81
A10		.65	25.4	2.54	5.08	15.24
A11		.65	25.4	2.54	8.89	7.62
A12		.59	25.4	2.54	10.16	5.08
B1	$[(\pm45)_{12}]_s$	.64	25.4	1.27	6.35	12.70
B2	↓	.64	25.4	2.54	6.35	12.70
B3		.64	25.4	2.54	7.62	10.16

[1]All specimens are 12.7 cm wide and are symmetric with respect to the horizontal centerline and the vertical centerline.

TABLE 2. MEMBRANE STIFFNESS AND FAILURE DATA FOR $[(\pm 30/90)_8]_s$ SPECIMENS

Specimen	EA, MN	Failure Stress, MPa	Failure strain, percent
A1	40.1	294	0.55
A2	38.5	255	.49
A3	39.3	244	.53
A4	36.6	202	.40
A5	35.8	178	.35
A6	40.1	292	.55
A7	39.1	286	.54
A8	38.7	244	.52
A9	37.4	275	.62
A10	35.4	200	.47
A11	36.6	223	.51
A12	37.2	240	.48

TABLE 3. FAILURE DATA FOR $[(\pm 45)_{12}]_s$ SPECIMENS

Specimen	Failure stress, MPa	Failure strain, percent
B1	175	1.63
B2	156	1.54
B3	153	1.48

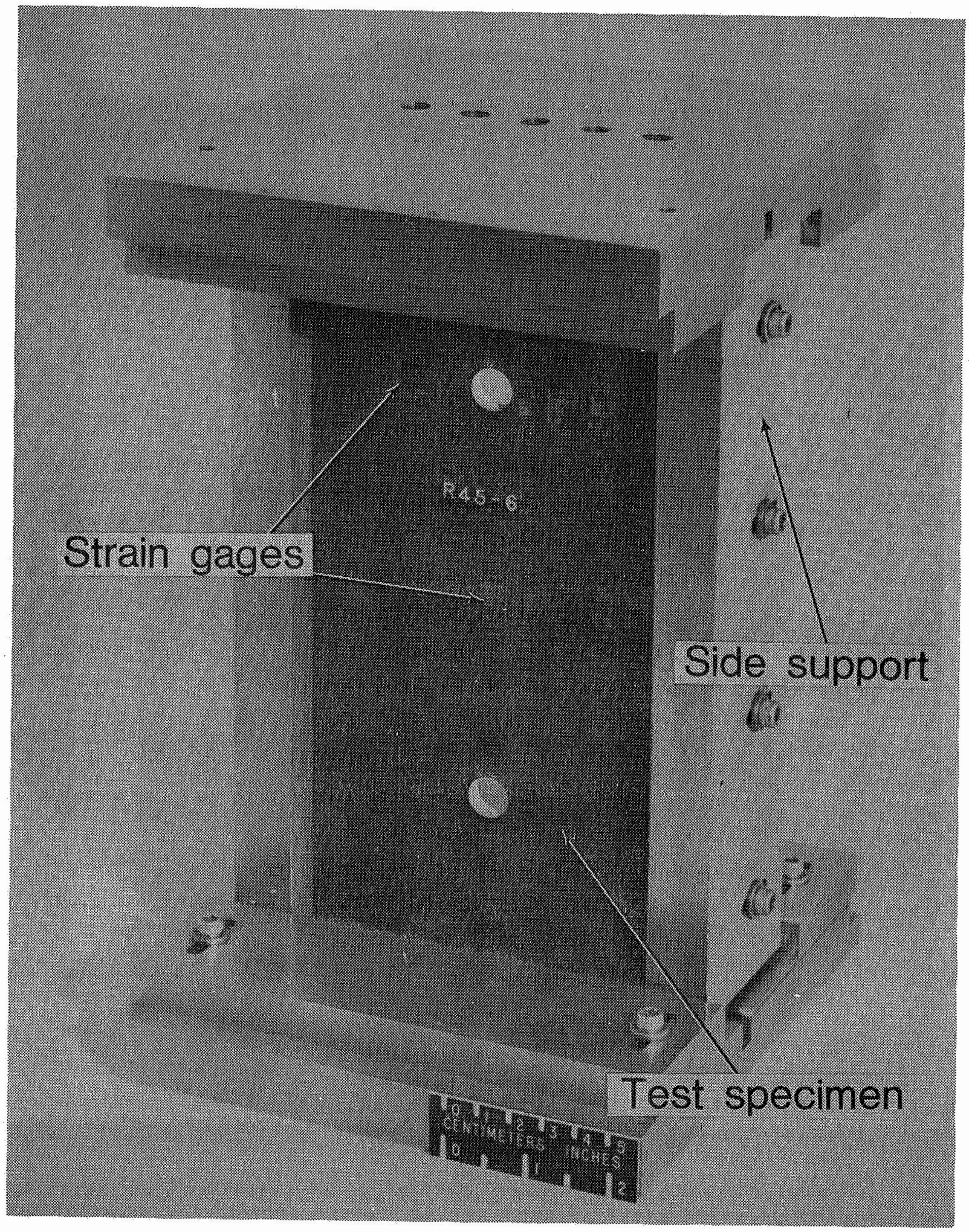

Figure 1. Typical specimen in test fixture.

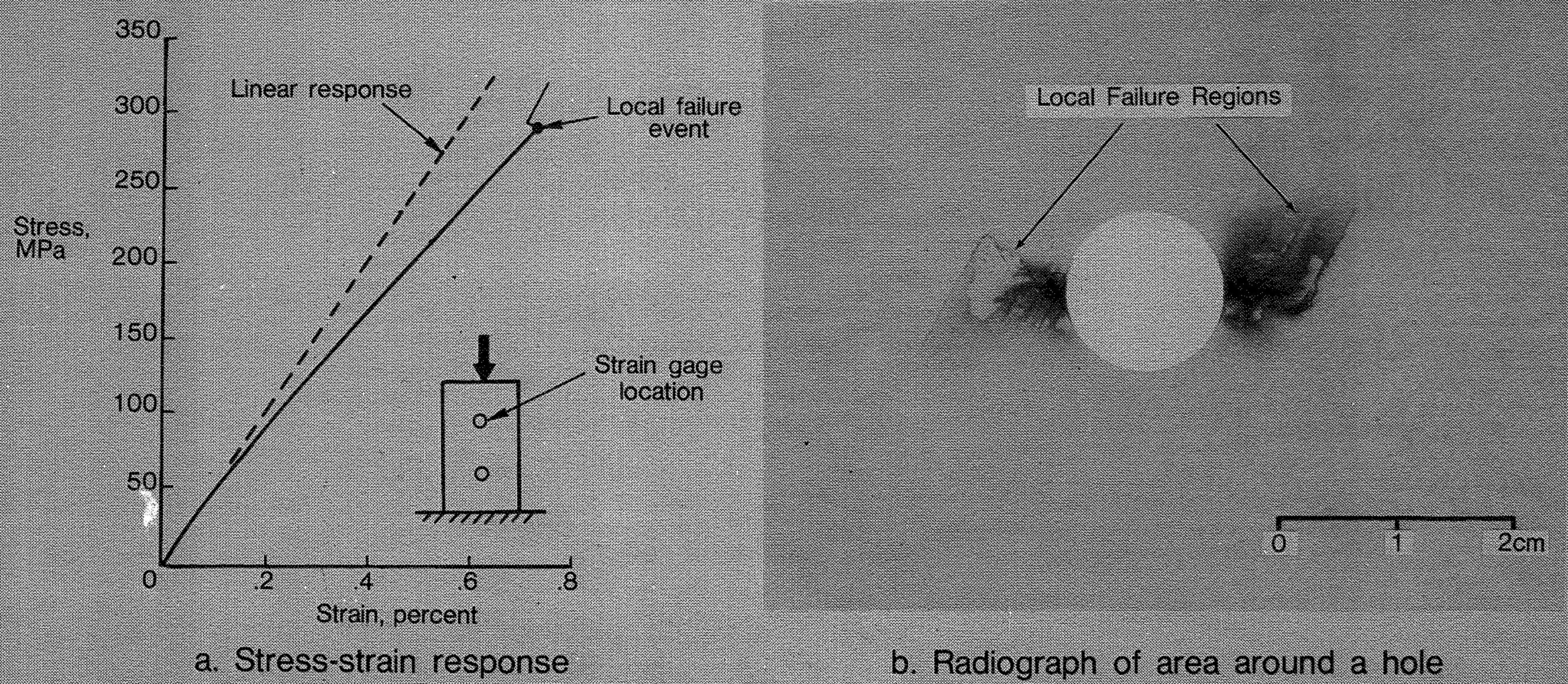

Figure 2. Stress-strain response and local failure of a $[(\pm 30/90)_8]_s$ laminate with two 1.27-cm-diameter holes.

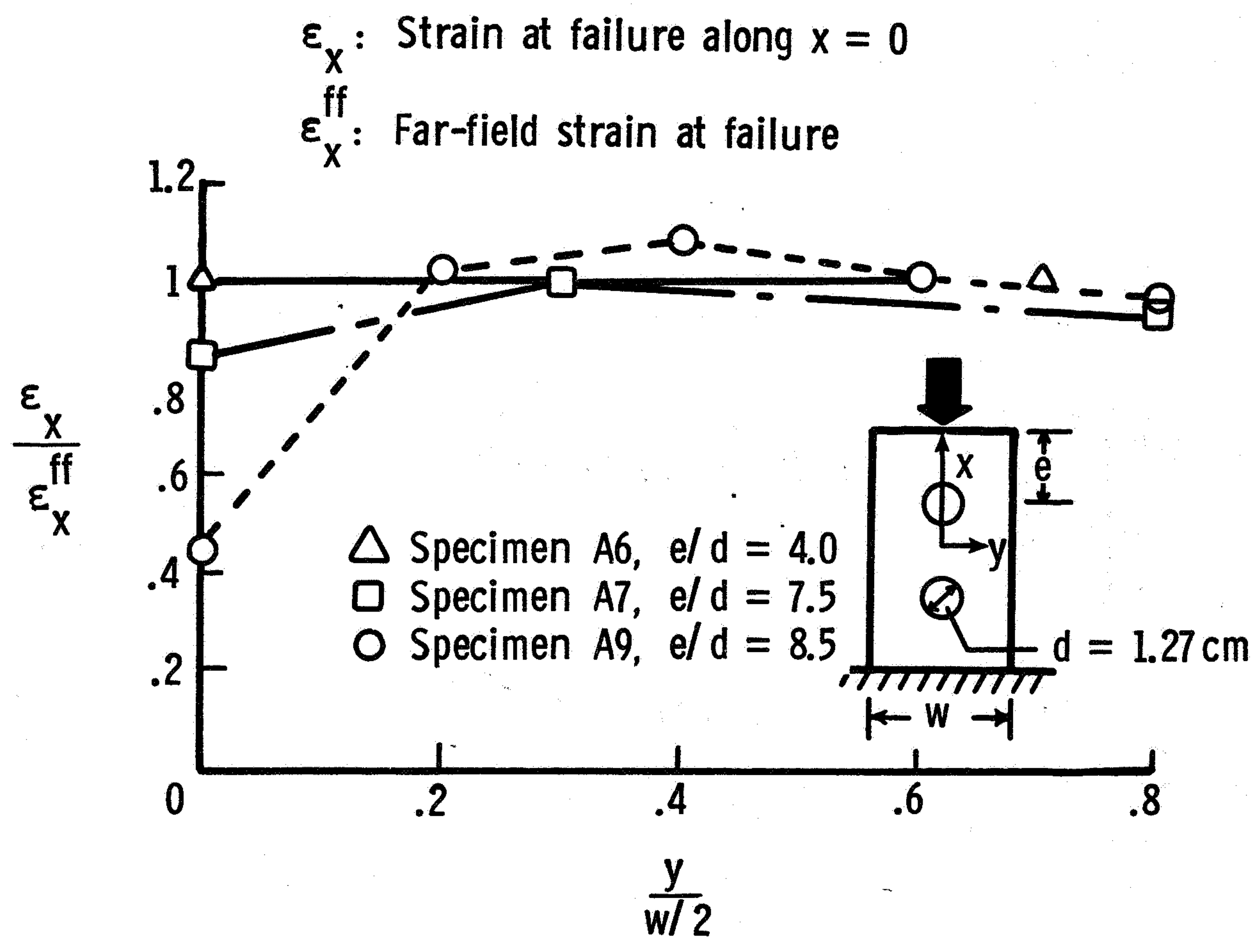

Figure 3. Axial strain along the y-axis (x = 0) for $[(\pm30/90)_8]_s$ laminates with two 1.27-cm-diameter holes.

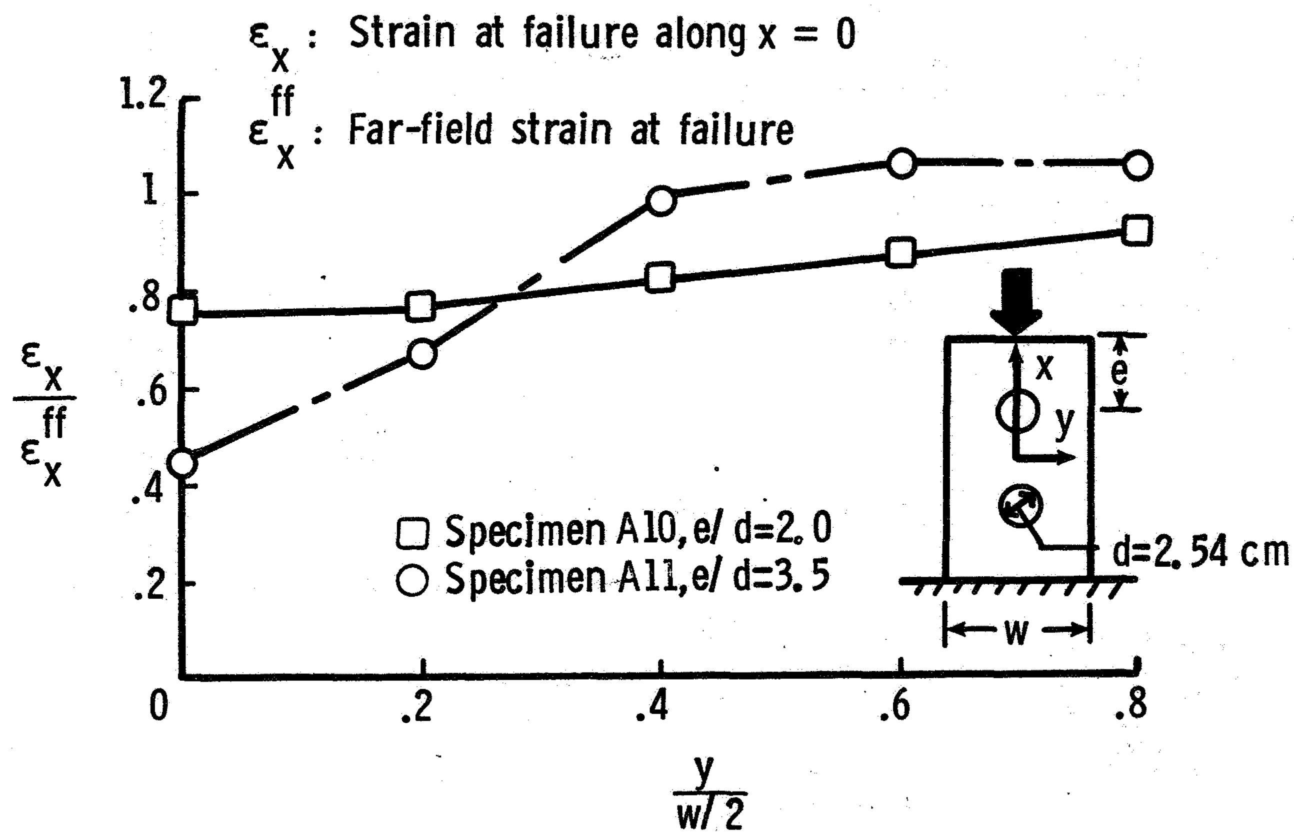

Figure 4. Axial strain along the y-axis (x = 0) for $[(\pm 30/90)_8]_s$ laminates with two 2.54-cm-diameter holes.

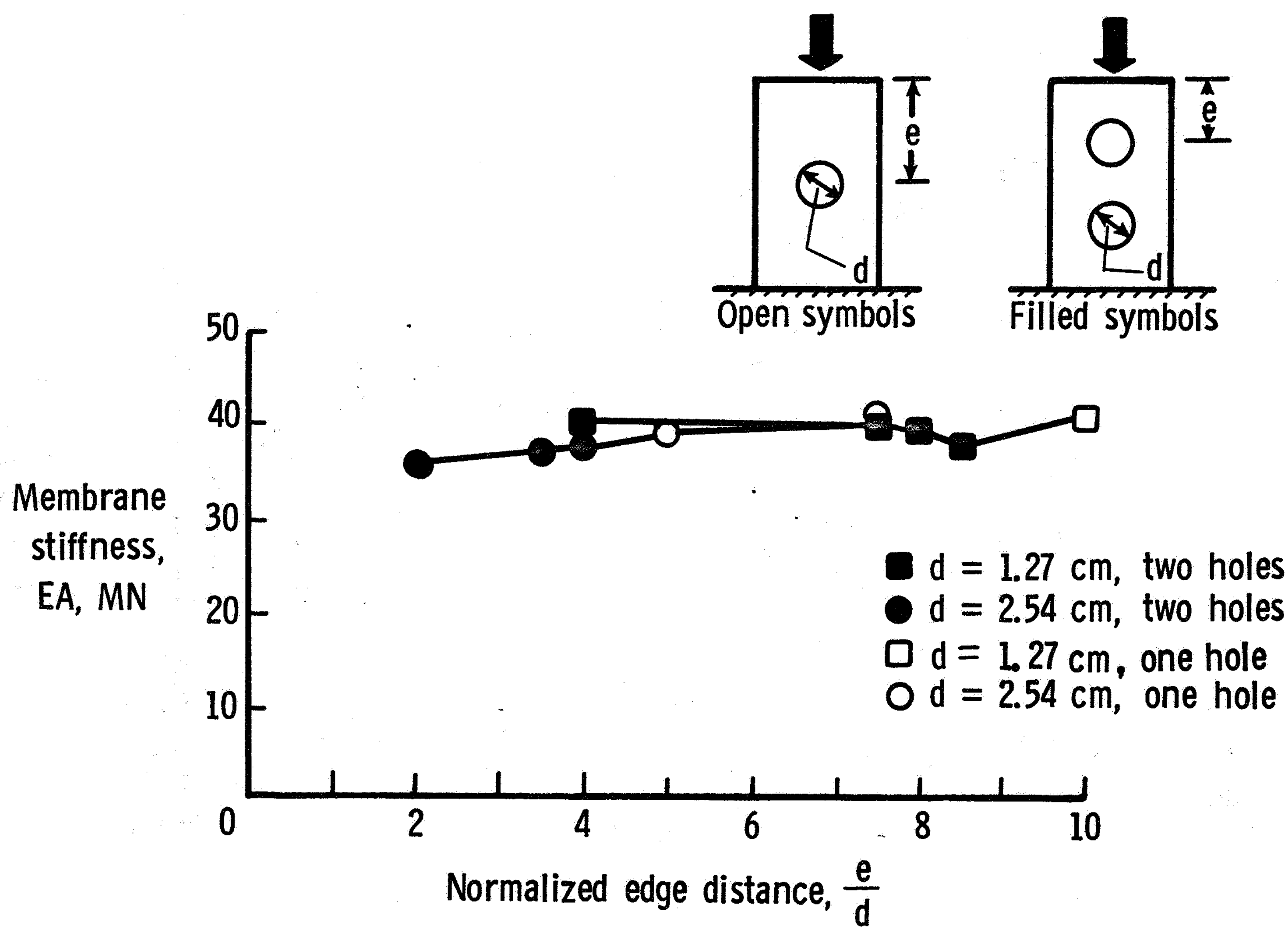

Figure 5. Membrane stiffness as a function of edge distance for $[(\pm 30/90)_8]_s$ laminates with holes.

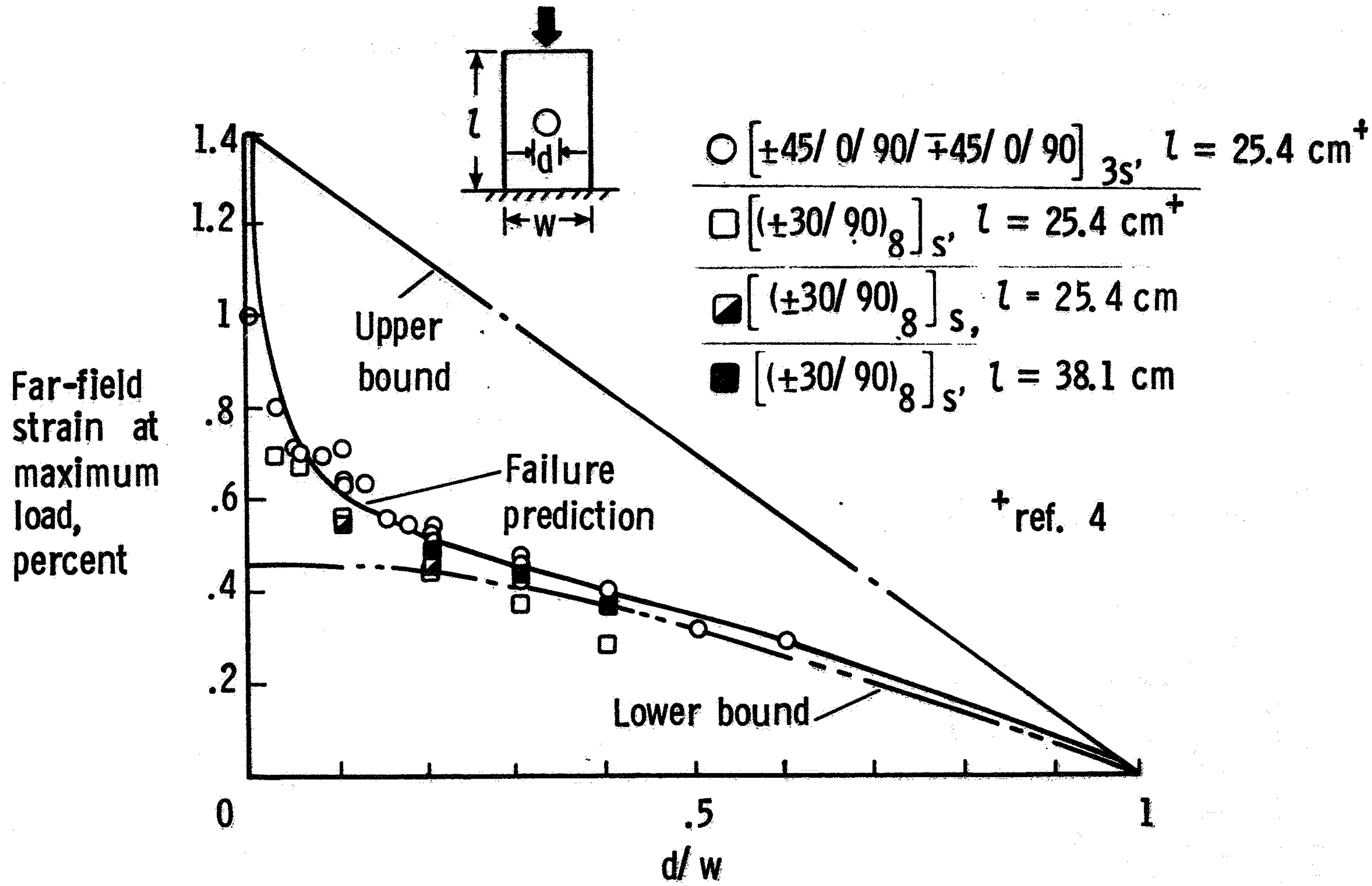

Figure 6. Far-field strain at maximum load as a function of hole diameter for quasi-isotropic laminates.

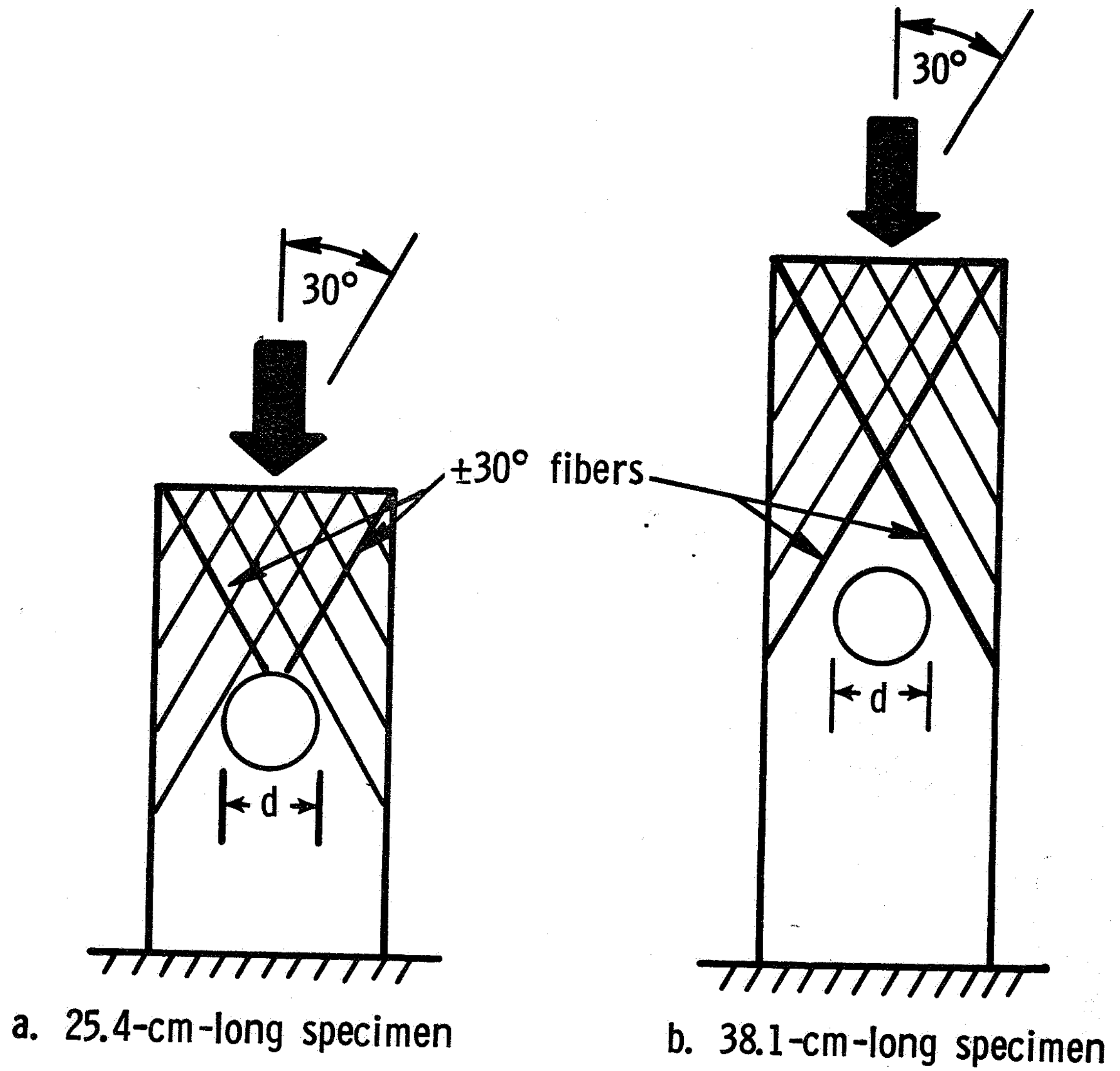

Figure 7. Fibers oriented at $\pm 30^{\circ}$ in $[\pm 30/90]_s$-class laminates with hole diameter d = 5.08 cm.

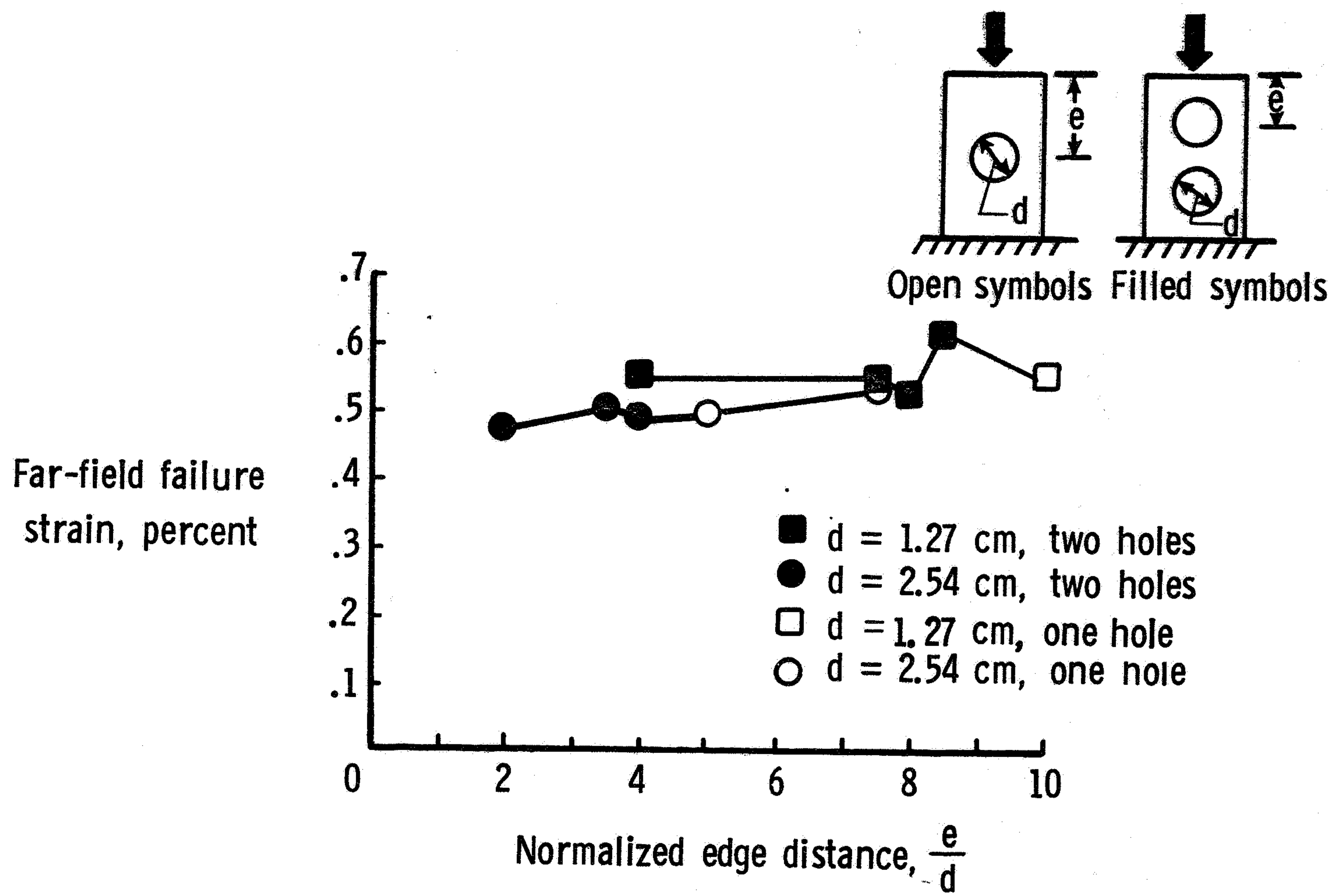

Figure 8. Failure strain as a function of edge distance for $[(\pm 30/90)_8]_s$ laminates with holes.

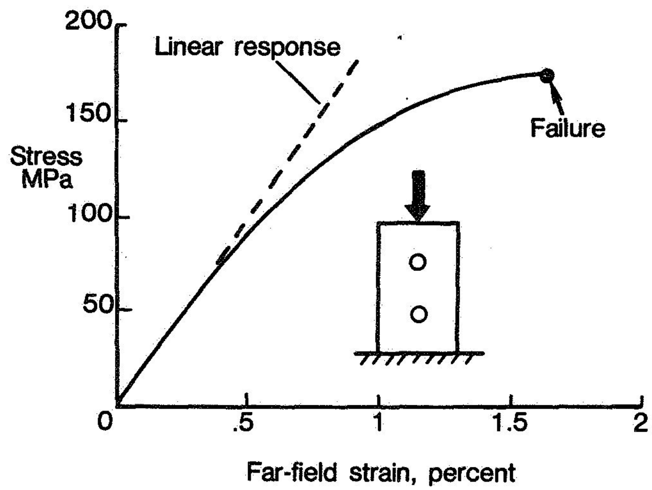

a. Stress-strain response

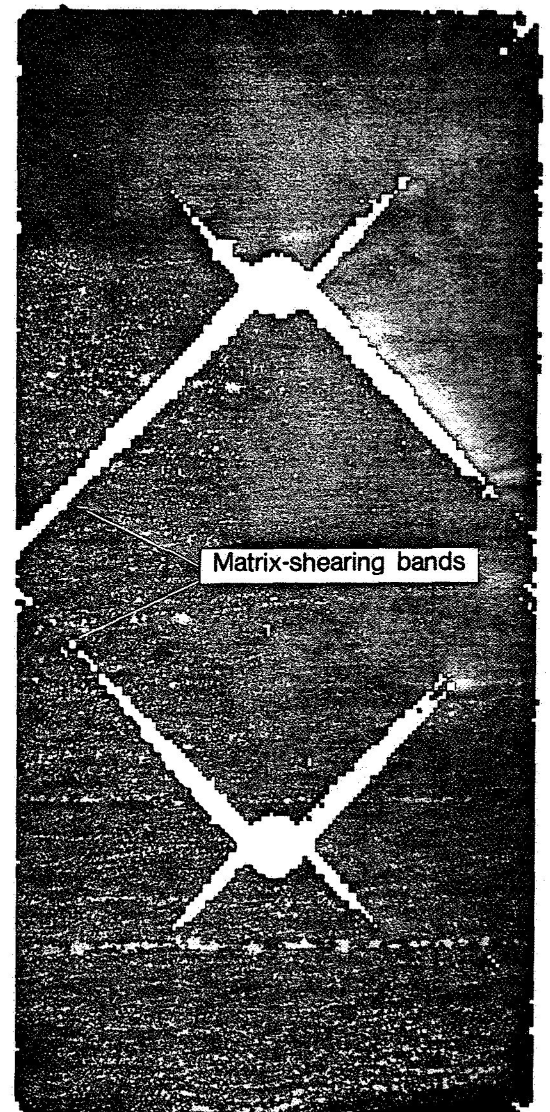

b. Photograph of C-span results for failed specimen

Figure 9. Stress-strain response and C-scan results for a $[(\pm45)_{12}]_s$ laminate with two 1.27-cm-diameter holes.

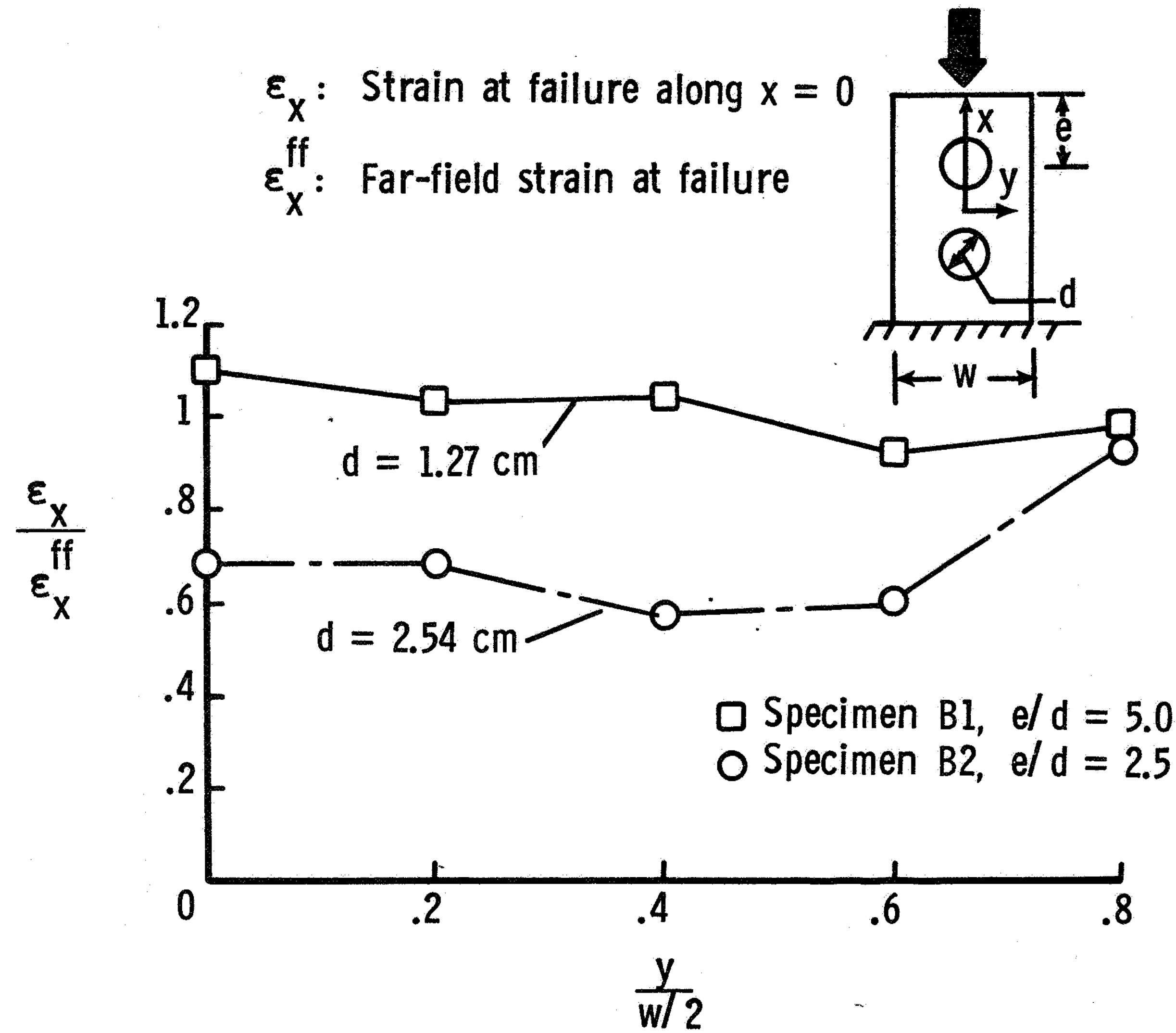

Figure 10. Axial strain along the y-axis ($x = 0$) for $[(\pm 45)_{12}]_s$ laminates with two holes.

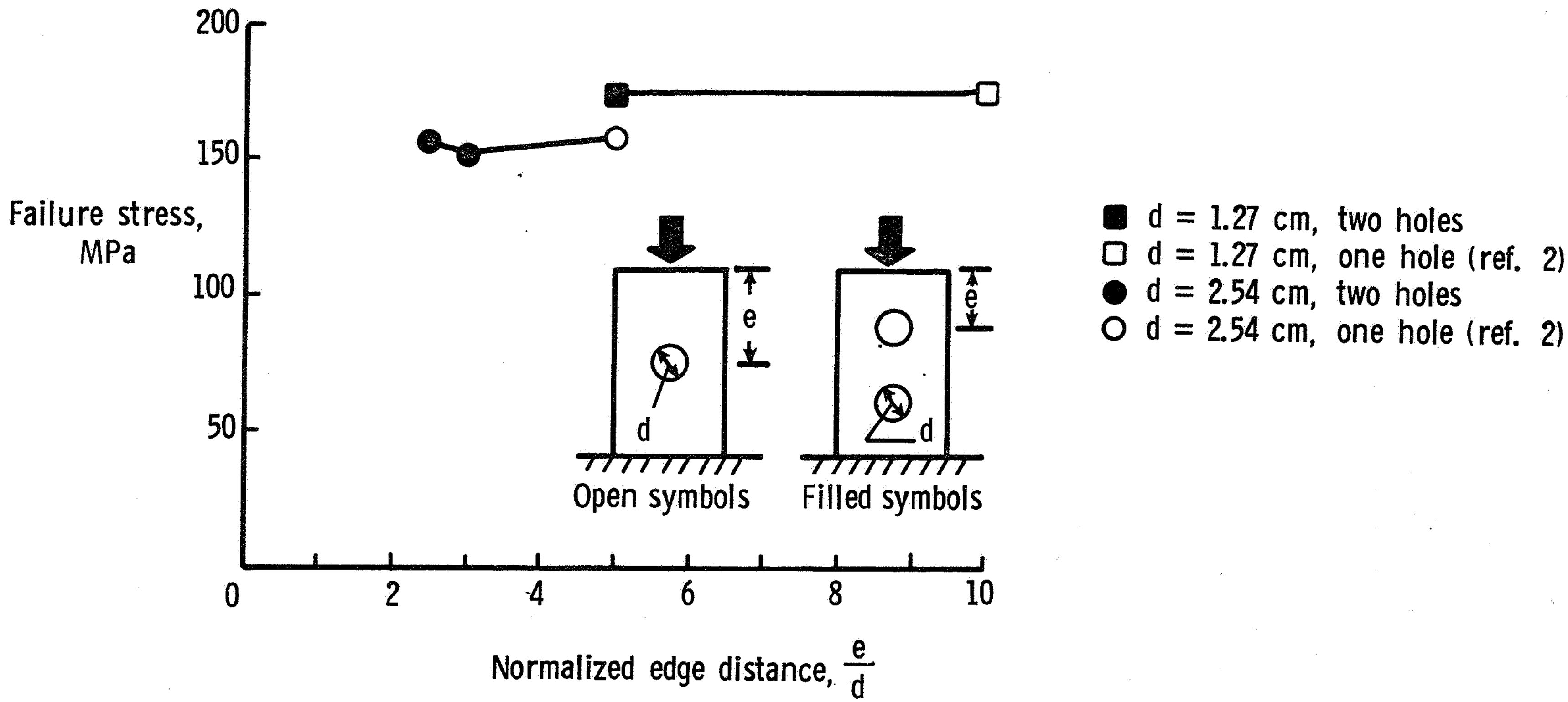

Figure 11. Failure stress as a function of edge distance for $[(\pm 45)_{12}]_s$ laminates with holes.

1. Report No.	2. Government Accession No.	3. Recipient's Catalog No.
NASA TM-86287		

4. Title and Subtitle	5. Report Date
Hole Interaction and Load Introduction Effects for Compression-Loaded Laminates with Holes	August 1984
	6. Performing Organization Code: 505-33-33-06
7. Author(s): Mark J. Shuart	8. Performing Organization Report No.
	10. Work Unit No.
9. Performing Organization Name and Address: NASA Langley Research Center, Hampton, VA 23665	11. Contract or Grant No.
	13. Type of Report and Period Covered: Technical Memorandum
12. Sponsoring Agency Name and Address: National Aeronautics and Space Administration, Washington, DC 20546	14. Sponsoring Agency Code

15. Supplementary Notes

Paper presented at the International Symposium on Composites: Materials and Engineering; Newark, Delaware; September 24-28, 1984

16. Abstract

An experimental investigation of a hole interaction effect and a load introduction effect for $[(\pm 30/90)_8]_s$ and $[(\pm 45)_{12}]_s$ laminates with holes was conducted. A hole interaction region was identified in some specimens, and this region was ineffective for carrying load. The membrane stiffness of a specimen with a hole interaction region is less than the membrane stiffness of a similar specimen without a hole interaction region. A load introduction effect that occurs on the sublaminate level was also observed. This effect can cause a nonuniform load diffusion into the interior of the specimen.

17. Key Words (Suggested by Author(s))	18. Distribution Statement
Compression Loading Graphite-Epoxy Laminates Circular Holes Composite Materials Hole Interaction Effect Load Introduction Effect	Unclassified - Unlimited Subject Category 24

19. Security Classif. (of this report)	20. Security Classif. (of this page)	21. No. of Pages	22. Price
Unclassified	Unclassified	26	A03